Article

Promotion of DNA Adsorption onto Microplastics by Transition Metal Ions

Lyuyuan Wu, Kshiti Patel, Mohamad Zandieh [ID] **and Juewen Liu** *[ID]

Department of Chemistry, Waterloo Institute for Nanotechnology, University of Waterloo,
200 University Avenue West, Waterloo, ON N2L 3G1, Canada
* Correspondence: liujw@uwaterloo.ca

Abstract: Microplastics can adsorb and spread a variety of pollutants in the ecosystem posing a threat to human health. One of the common pollution sources of environmental waters is metal ions, which not only adsorb on microplastics but can also promote the adsorption of other invasive species such as environmental DNA. Recently, we showed that environmentally abundant metal ions (Na^+, Mg^{2+} and Ca^{2+}) can promote the adsorption of single-stranded DNA (ssDNA) onto microplastics. Herein, we investigated the effect of transition metal ions including Zn^{2+} and Mn^{2+} and compared them with Mg^{2+} for promoting DNA adsorption. To better mimic environmental DNA, we also used a salmon sperm double-stranded DNA (dsDNA) (~2000 bp). For both ssDNA and dsDNA, the transition metals induced a higher adsorption capacity compared to Mg^{2+}, and that correlated with the higher binding affinity of transition metals to DNA. Although metal-mediated interactions were vital for ssDNA adsorption, the dsDNA adsorbed on the microplastics even in the absence of metal ions, likely due to the abundance of binding sites of the 100-times longer dsDNA. Finally, desorption studies revealed that hydrophobic interactions were responsible for dsDNA adsorption in the absence of metal ions.

Keywords: microplastics; DNA; adsorption

1. Introduction

Annual plastic production is approximately 400 million metric tons [1], and the global plastic market is worth more than USD 500 billion. Such popularity is because plastics are durable, cheap, and highly versatile. However, due to low biodegradability, plastic pollution is considered as one of the major environmental issues [2].

Microplastics are submillimeter plastic particles with a high surface-to-volume ratio, which are divided into two types: (1) primary microplastics, which are plastic beads manufactured to be used in commercial goods such as detergents and cosmetics, and (2) secondary microplastics, which are generated when plastic wastes are shredded into submillimeter particles in the environment via mechanical force, chemical reactions and/or microbiological degradation [3]. Microplastics in the environment adsorb a variety of pollutants ranging from heavy metal ions [4] to invasive living organisms [5]. In addition, microplastics are internalized by fish, birds, and other animals, and can pass through the food chain to reach human beings. It was estimated that each individual on average consumes an equivalent of a credit card worth (~5 g) of microplastics per week through ingestion and inhalation [6]. This poses a serious threat to human health, since microplastics can stimulate infertility, immune system disorders and even cancer [7,8].

Transition metal ions such as zinc (Zn^{2+}) and manganese (Mn^{2+}) exist in many environmental water bodies. Studies on the adsorption of these metal ions by microplastics have been performed [9–11]. For example, Hildebrandt et al. systematically compared the adsorption of 55 metal and metalloid ions on a couple of microplastic materials at neutral pH [9]. They observed that the adsorbed metals were released at a low pH when

gastrointestinal chemistry was mimicked; thereby, possible detrimental impacts on the food chain and human health were proposed. In another instance, Zhang et al. studied the adsorption of five different mono- and divalent metal ions on polystyrene nanoplastics [11] by investigating the aggregation kinetics of plastic particles, which were induced due to the charge neutralization upon metal adsorption. They used transmission electron microscopy (TEM) and energy-dispersive X-ray (EDX) spectroscopy to confirm the adsorption behavior of metal ions and highlighted the environmental impacts of metal ion adsorption on nanoplastics. Most previous studies focused on toxicity in organisms [12], while the molecular level effect on biomolecular interactions was rarely studied. For instance, metal ions are known to bind with DNA at various binding sites with different affinities [13]. At the same time, metal ions can be adsorbed to various nanomaterials such as graphene oxide, polydopamine and nanocellulose [14,15]. Therefore, metal-mediated interactions can result in the adsorption of DNA on a variety of nanomaterials [16–18].

We recently reported that environmentally abundant metal ions such as sodium (Na^+), magnesium (Mg^{2+}) and calcium (Ca^{2+}) can promote the adsorption of DNA oligonucleotides onto microplastics [19]. Deoxyribonucleic acid (DNA) is a highly important biomolecule, and the investigation of DNA adsorption onto microplastics helps the better comprehension of the nature of interactions between environmental DNA and microplastics. Moreover, it provides insights for future DNA aptamer selection for microplastics and related biosensors [20–23]. However, the effect of metal ions on the adsorption of long biological DNA is unknown, and those DNA species are more environmentally and biologically relevant. In this work, we focus on the effect of transition metals including Zn^{2+} and Mn^{2+} on the adsorption of both single-stranded (ssDNA) and double-stranded DNA (dsDNA) on microplastics. The ssDNA adsorption studies could mimic how DNA aptamers might interact with microplastics, while the dsDNA is relevant to the interaction of environmental DNA with microplastics.

2. Materials and Methods

2.1. Materials

The 21-mer ssDNA (5′-AAA AAA AAA CCC AGG TTC TCT-3′) with a 3′-FAM label, and the two complementary 24-mer ssDNAs (5′-CCC AGG TTC TCT TCA CAG ATG CGT-3′ and 5′-ACG CAT CTG TGA AGA GAA CCT GGG-3′) were purchased from Integrated DNA Technologies (IDT, Coralville, IA, USA). Low molecular weight DNA from salmon sperm (~2000 bp), various metal chloride salts, ethylenediaminetetraacetic acid (EDTA) and dimethyl sulfoxide (DMSO) were obtained from Sigma-Aldrich. Urea and 4-(2-hydroxyethyl) piperazine-1-ethanesulfonic acid (HEPES) were from Mandel Scientific (Guelph, ON, Canada). Agarose M and 10 TBE (Tris-borate-EDTA) buffer were from Bio Basic (Markham, ON, Canada). Milli-Q water was used for preparing all the buffers and solutions.

2.2. Preparation of Microplastics

Three commonly used plastic items including a water bottle, a plastic sheet and a plastic spoon were collected. Their composing materials were, respectively: polyethylene terephthalate (PET), polyvinylchloride (PVC) and polystyrene (PS). To remove organic residues, the plastics were then washed with ethanol in a sonication bath for 5 min. Finally, the plastics were shredded into microplastics using a steel kitchen cheese grater. To eliminate the effects of aging or wetting of microplastics, the microplastics were dried at room temperature under vacuum and were dispersed in water right before the adsorption experiments.

2.3. Purification of Salmon Sperm DNA

The as-received salmon sperm DNA may contain impurities since they were extracted from biological samples. To purify salmon dsDNA, the ethanol precipitation method was used. In this method, 5 mg of salmon sperm DNA powder was dissolved in 60 µL

sodium acetate (3 M, pH 5.2) followed by the addition of 600 μL 100% ethanol. The sample was then placed in a freezer (-20 °C) for 3 h. After that, the solution was centrifuged (15,000 rpm, 30 min) at 4 °C, and washed with cold 70% ethanol (stored at 4 °C) three times. The purified DNA was dissolved in buffer (10 mM HEPES, pH 7.6) before use.

2.4. Adsorption of ssDNA and Salmon dsDNA

The purified salmon sperm dsDNA (1 μM) was first stained by $2\times$ SYBR Green I (SGI). Note that $1\times$ SGI has a concentration of 2 μM. Then, 10 nM FAM-labelled ssDNA (DNA strand concentration) or 1 μM salmon sperm dsDNA (DNA base concentration) was mixed with 500 μg/mL of PET, PVC, or PS microplastics in the presence of different concentrations of metal ions (Mg^{2+}, Mn^{2+}, or Zn^{2+}) in a buffer (10 mM HEPES, pH 7.6). The concentration of microplastics was optimized to be high enough to ensure that the surface capacity was not a limiting factor for the DNA adsorption. To avoid the precipitation of microplastics, the samples were agitated gently during the reaction. After 1 h, the samples were centrifuged (1000 rpm, 2 min), and the fluorescence intensity (Ex: 485 nm; Em: 535 nm) of the supernatant was measured and compared to a control sample (devoid of microplastics) to calculate the adsorbed DNA. To test the dsDNA adsorption in wastewater instead of buffer, a wastewater sample was obtained from Kitchener Wastewater Treatment Plant (Kitchener, ON, Canada). The supernatant of wastewater sample was clear after the centrifugation (1000 rpm, 2 min) to minimize its impact on the fluorescence intensity measurements (Figure S1).

2.5. Adsorption of Short dsDNA

First, the 24-mer duplex DNA was prepared. The two complementary ssDNA (24-mer, 100 nM each) were heated at 95 °C for 2 min, and then slowly cooled to room temperature over a time course of 2 h to achieve hybridization and formation of dsDNA. Then, the short dsDNA was stained with SGI ($2\times$) and mixed with 500 μg/mL PET microplastics in the presence of different concentrations of Zn^{2+} in buffer (10 mM HEPES, pH 7.6). Finally, after 1 h incubation, the samples were centrifuged (1000 rpm, 2 min), and the fluorescence intensity (Ex: 485 nm; Em: 535 nm) of the supernatant was measured and compared to a control sample (devoid of microplastics) to calculate the percentage of the adsorbed short dsDNA.

2.6. Desorption of DNA from Microplastics

First, 1 μM of dsDNA was adsorbed on PET, PVC or PS as described above in the presence of 0 mM or 1 mM Zn^{2+} for 1 h to achieve adsorption. Then, the microplastics were separated from the solution. Totals of 4 M urea, 10 mM EDTA, or 25% DMSO were mixed with the microplastics for 1 h keeping the buffer conditions the same as the adsorption experiment. Finally, the supernatant of the samples was collected by centrifugation (1000 rpm, 2 min), and the fluorescence intensity enhancement of the supernatant was measured to quantify the desorbed dsDNA.

3. Results and Discussion

### 3.1. Preparation and Characterization of the Microplastics

Three plastic objects composed of some common plastic materials were collected including a water bottle, a plastic sheet, and a plastic spoon. Based on their Raman spectra collected using a 785 nm laser excitation, the composing materials were identified to be PET, PVC and PS, respectively (Figure 1A–C) [24]. To mimic environmental microplastics, the plastic objects were shredded mechanically using a kitchen grater, and their size and morphology were observed under an optical microscope. As shown in Figure 1D–F, the size distribution of the prepared microplastics was from 20 μm to 800 μm and thus they fit the definition of microplastics (<1 mm), and the morphology was a combination of microscale fibers and fragments.
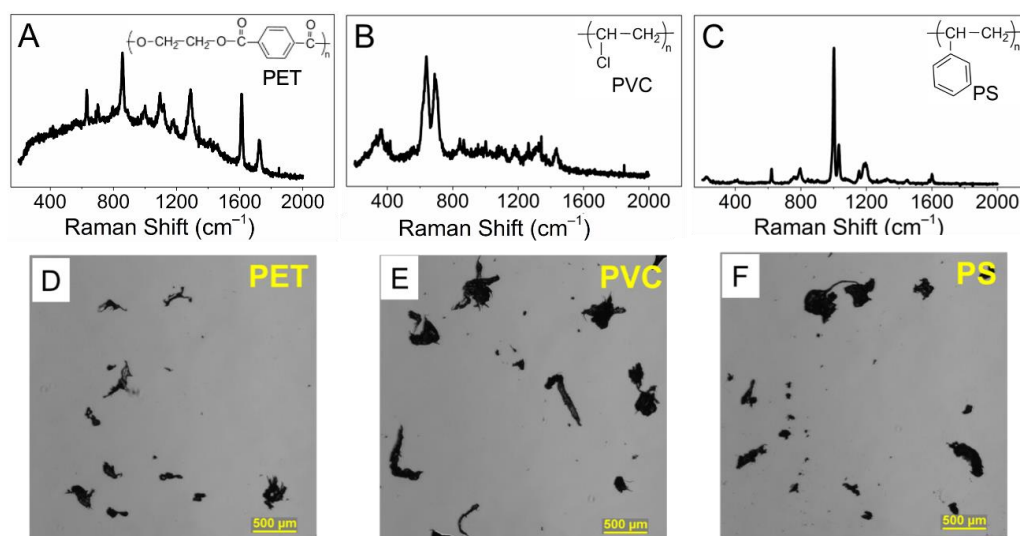
Figure 1. Raman spectra and molecular structures of the plastic items in this work: (**A**) a water bottle (PET), (**B**) a plastic sheet (PVC) and (**C**) a plastic spoon (PS). Optical microscope images of the (**D**) PET, (**E**) PVC and (**F**) PS microplastics prepared by grating the plastic items.

3.2. Comparison of Mg^{2+}, Mn^{2+} and Zn^{2+} for ssDNA Adsorption

At pH 7.6, the PET, PVC, and PS microplastics were all negatively charged based on zeta-potential measurement (Figure 2A), thereby repelling negatively charged DNA. To screen the charge repulsion and bridge the interactions between DNA and the microplastics, metal ions or salt can be used [16].
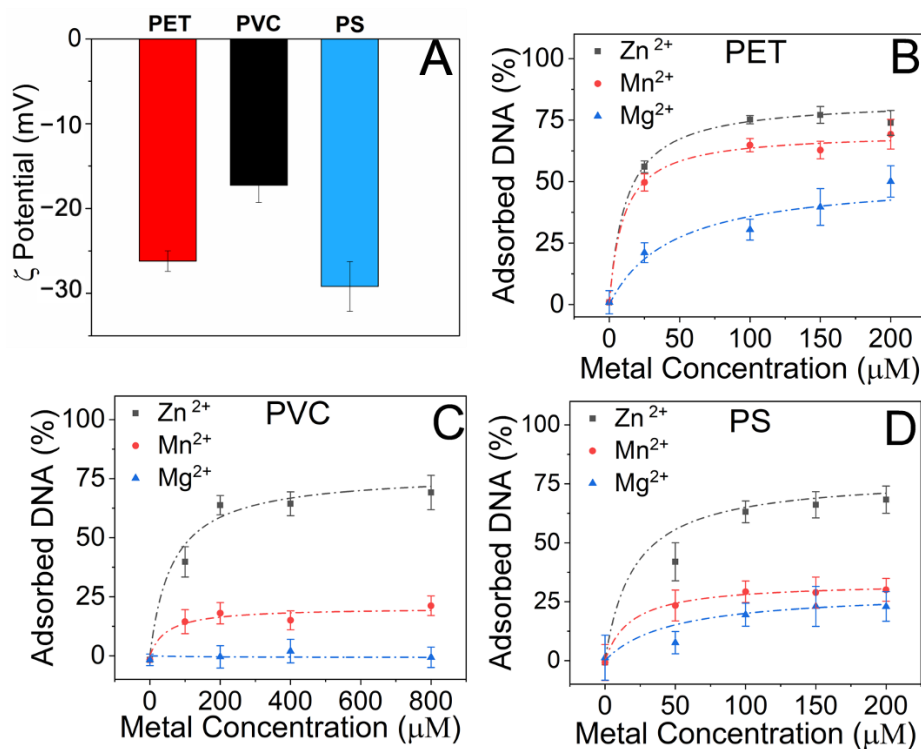
Figure 2. (**A**) ζ-Potentials of the three microplastic samples in a buffer (10 mM HEPES, pH 7.6). They are all negatively charged. Adsorption of 10 nM ssDNA onto 500 µg/mL of: (**B**) PET, (**C**) PVC, or (**D**) PS microplastics in the presence of different concentrations of Zn^{2+}, Mn^{2+}, or Mg^{2+}.

To study DNA adsorption, a FAM-labeled 21-mer ssDNA was first used, and the amount of DNA adsorption was quantified by measuring the fluorescence intensity of the supernatant. First, the adsorption of the ssDNA on the PET microplastics was investigated in the presence of transition metal ions such as Mn^{2+} and Zn^{2+} and a comparison was made with an environmentally abundant metal ion, Mg^{2+}.

With increasing metal ion concentration, ssDNA adsorption on PET was promoted with all the three metals (Figure 2B). The data fitted well with a single-site binding model, where the adsorbed DNA concentration has a hyperbolic saturable dependence on the concentration of free metal ions [25]. Therefore, the metal concentration at which the adsorbed DNA reaches half-saturation (K) was calculated for each metal ion. The K value for Mn^{2+} and Zn^{2+} was ~10 μM. In contrast, in the presence of 200 μM Mg^{2+}, only ~50% of the DNA was adsorbed and saturation was not achieved at this point. By adding a much higher concentrations of Mg^{2+} (2 mM), we recently calculated the K value of Mg^{2+} for the adsorption of the same DNA on PET to be ~60 μM [19]. The smaller K values of Mn^{2+} and Zn^{2+} suggested that the transition metal ions are more efficient in promoting ssDNA adsorption on PET microplastics.

We also tested the ssDNA adsorption on PVC microplastics in the presence of the same metal ions. Interestingly, no adsorption was observed in the presence of up to 800 μM Mg^{2+}, and only 20% of the DNA was adsorbed in the presence of 800 μM Mn^{2+} (Figure 2C). On the other hand, Zn^{2+} was efficient in promoting DNA adsorption on PVC. Adsorption saturation on PVC occurred at 75% of the initial DNA concentration when 800 μM Zn^{2+} was used. The adsorption on PS was also the highest (~75%) when 200 μM Zn^{2+} was added (Figure 2D), whereas only ~25% of DNA adsorption occurred in the presence of Mn^{2+} or Mg^{2+}.

Overall, the data suggested that the ssDNA adsorption efficiency follows the order of PET > PS > PVC. This can be explained by the aromatic rings in the PET and PS structures, which can provide extra attractive forces such as hydrogen bonding and π–π stacking for DNA adsorption [19,26,27]. Moreover, the efficiency of metal ions in promoting DNA adsorption followed the order of $Zn^{2+} > Mn^{2+} > Mg^{2+}$. This trend correlated with metal ion affinity to both the phosphate backbone and nucleobases of DNA [13,28,29]. Therefore, the transition metal ions were likely to have specific interactions with DNA instead of simply serving as a charge screening role. Otherwise, all the divalent metal ions should have a similar effect in promoting DNA adsorption.

3.3. Adsorption of dsDNA

We then tested the adsorption of dsDNA, which is more relevant to environmental conditions, where genomic DNA from microbes might be adsorbed by microplastics [30,31]. Salmon sperm dsDNA (~2000 base pairs) was first purified using the ethanol precipitation method. To assess the purity of DNA, the UV-vis spectrum of the sample was acquired, and the absorbance was measured at 230, 260 and 280 nm [32]. The 260/280 ratio was 1.81 and the 260/230 ratio was 2.24 (Figure S2). Both values confirmed that the dsDNA was successfully purified, and the sample was devoid of protein and other organic contaminations [33]. The purified dsDNA was then stained by SYBR Green I (SGI) to allow the highly sensitive quantification of adsorption using fluorescence spectroscopy (Figure S3). This quantification method is more sensitive than DNA absorbance measurement at 260 nm.

First, the effect of Zn^{2+} on the dsDNA adsorption onto different microplastics was studied. Interestingly, even in the absence of metal ions, the PS and PET microplastics already adsorbed ~65% and ~80% of the dsDNA, respectively (Figure 3A). As shown above, metal ions were vital for the adsorption of ssDNA onto microplastics. The affinity of dsDNA for microplastics in the absence of metal ions implied a different adsorption mechanism from ssDNA. One fundamental difference between these two structures is that the nucleobases are not exposed in dsDNA, which is the reason why ssDNA has higher adsorption affinity than dsDNA to nanomaterials such as graphene oxide and polydopamine [28,34].
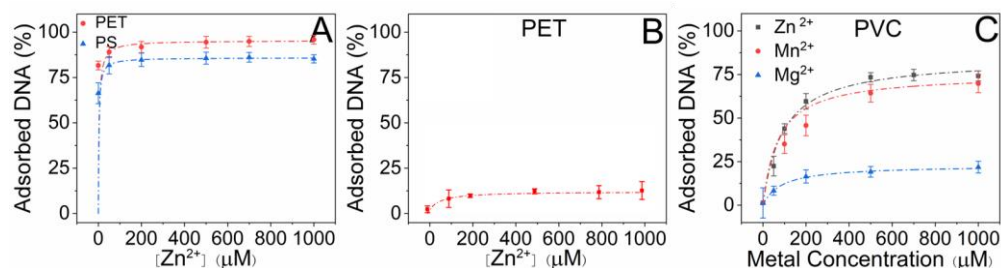
Figure 3. (**A**) Adsorption of 1 μM (DNA base concentration) salmon sperm dsDNA (~2000 bp) onto 500 μg/mL of PS and PET microplastics in the presence of different concentrations of Zn^{2+} in a buffer (10 mM HEPES, pH 7.6). (**B**) Adsorption of 100 nM short dsDNA (24 bp) onto 500 μg/mL of PET microplastics in the presence of different concentrations of Zn^{2+} in a buffer (10 mM HEPES, pH 7.6). (**C**) Adsorption of 1 μM salmon sperm dsDNA (~2000 bp) onto 500 μg/mL of PVC microplastics in the presence of different concentrations of various metal ions in a buffer (10 mM HEPES, pH 7.6).

On the other hand, it should also be considered that the salmon sperm dsDNA used here is remarkably longer (2000 bp) than the ssDNA oligonucleotides used (21-mer). To compare the effect of length, we then tested the adsorption of a short dsDNA (24 bp) on PET at different concentrations of Zn^{2+}. Polyethylene terephthalate was chosen as the most efficient microplastic material [19], and Zn^{2+} was chosen as the most efficient metal ion to reveal the highest short dsDNA adsorption efficiency. As shown in Figure 3B, unlike the salmon sperm dsDNA, no adsorption of the short dsDNA occurred in the absence of metal ions. Moreover, only ~10% was adsorbed in the presence of 1 mM Zn^{2+}, which was reasonable based on the expected lower affinity of dsDNA to nanomaterials (e.g., the DNA bases are shielded in dsDNA) [28,34]. Therefore, the adsorption of the salmon dsDNA in the absence of metal ions was attributed to the remarkably higher number of binding sites (~100-fold). The abundance of binding sites may amplify the individually weak interactions and result in a stable adsorption through polyvalent binding [35].

Further, the adsorption of salmon sperm dsDNA was also achieved on PVC in the presence of Zn^{2+} or Mn^{2+} and reached 75% in the presence of 1 mM metal ion (Figure 3C, black and red curves). On the other hand, only a slight adsorption was achieved with up to 1 mM of Mg^{2+} (Figure 3C, blue curve). The data fitted well to the single-site binding model, and the *K* values were calculated to be 109 μM, 3.8 μM and 2.5 μM of Zn^{2+} for adsorption on PVC, PET, and PS, respectively. Therefore, similar to ssDNA, PET and PS showed a remarkably higher affinity (~40-fold) than PVC to dsDNA in the presence of Zn^{2+}.

3.4. Desorption of dsDNA to Probe Adsorption Affinity

To gain more insights into the nature of interactions between microplastics and dsDNA, we then performed desorption studies. Totals of 10 mM EDTA, 4 M urea and DMSO (25%) were, respectively, added to probe metal-mediated interactions, hydrogen bonding and hydrophobic interactions. In the absence of Zn^{2+}, ~85% of DNA was desorbed by DMSO from PET and PS (Figure 4A,B), while only up to ~20% desorption was induced by urea. Therefore, it was suggested that dsDNA was adsorbed through hydrophobic interactions onto PET and PS in the absence of metal ions.

When DNA was adsorbed in the presence of 1 mM Zn^{2+}, the desorption induced by DMSO remarkably decreased to ~25% for PET and PS. In contrast, more DNA was desorbed by EDTA (up to 30%). It was suggested that in the presence of Zn^{2+}, the role of hydrophobic interactions reduced and instead, metal-mediated interactions came into play. Therefore, the conformation of DNA was likely to be different in the presence and absence of Zn^{2+}. Moreover, in the presence of metal ions, the overall desorption was decreased suggesting a tighter binding. Metal ions could also make the surface charge of the microplastics less negative (compare Figures S4 and 2A); thereby, the adsorption of negatively charged DNA would be more electrostatically favorable.
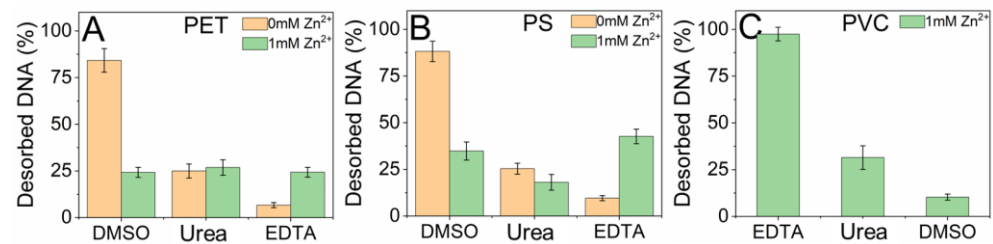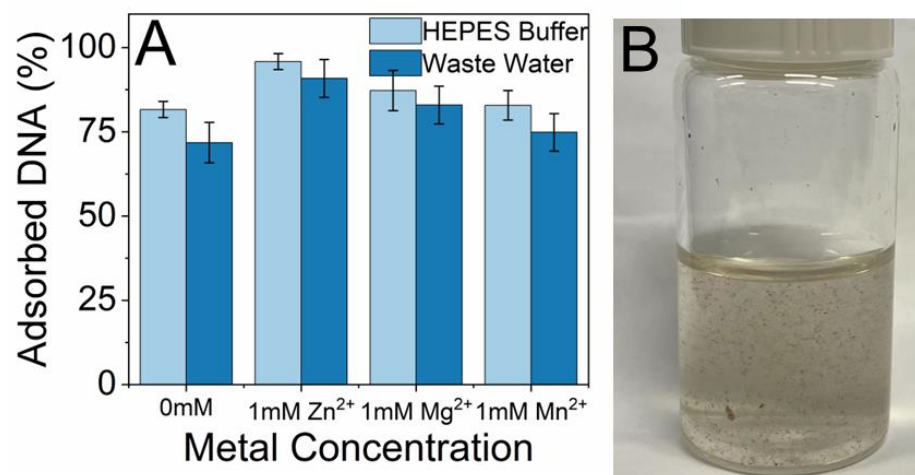
Figure 4. The desorption of salmon sperm dsDNA (~2000 bp) induced by DMSO (25%), 4 M urea, or 10 mM EDTA from the (**A**) PET, (**B**) PS, or (**C**) PVC microplastics. The pre-adsorption and desorption experiments were performed in a buffer (0 or 1 mM Zn^{2+}, 10 mM HEPES, pH 7.6).

For PVC, the desorption was studied after adsorption in the presence of 1 mM Zn^{2+}. When EDTA was added, dsDNA was almost fully desorbed (Figure 4C), suggesting that metal-mediated interactions are vital for dsDNA adsorption on PVC. These data agreed with the adsorption experiments, where dsDNA did not adsorb on PVC in the absence of Zn^{2+} (Figure 3C, black curve). Moreover, for different microplastics, the comparison of EDTA-induced desorption at the same Zn^{2+} concentration (1 mM) suggested that the dsDNA adsorption affinity followed the order of PET > PS > PVC.

3.5. Testing DNA Adsorption in Wastewater

Finally, we tested the adsorption of the salmon sperm dsDNA on PET microplastics in real wastewater samples when various metal ions were added at 1 mM concentration (Figure 5A). No obvious change was observed compared to that in clean HEPES buffers; all achieved between 70% and 100% DNA adsorption, suggesting that the dsDNA adsorption on microplastics was stable against inhibition or displacement by other pollutants in the wastewater. A photograph of the wastewater used in this experiment is shown in Figure 5B, and this appeared to be a challenging sample containing a lot of contaminants and particulates. Nevertheless, they did not affect DNA adsorption. This observation supported the adsorption of biological DNA onto microplastics in environmental waters [30,31].

Figure 5. (**A**) Adsorption of 1 μM salmon sperm dsDNA (~2000 bp) onto 500 μg/mL of PET microplastics in the absence/presence of 1 mM of various metal ions in wastewater or a buffer (10 mM HEPES, pH 7.6). (**B**) A photograph of the wastewater sample used in this study.

3.6. Additional Discussion

In this work, we discovered that long double-stranded DNA can be adsorbed to various microplastics with little help from divalent metal ions. In contrast, short single-stranded oligonucleotides require divalent metals for the adsorption, especially for plastics

without aromatic structural units such as PVC. Transition metal ions are more effective to promote DNA adsorption compared to alkaline earth metals such as Mg^{2+}. This can be attributed to their stronger interaction with DNA.

The adsorption of DNA can also be enhanced by densely immobilizing DNA oligonucleotides on gold nanoparticles forming spherical nucleic acids, which was demonstrated in our previous work [19]. A common feature of long double-stranded DNA and spherical nucleic acids is that they both have more contacting points to microplastics compared to short DNA oligos. Spherical nucleic acids may not have potent biological functions, but they may serve as probes to study the property of microplastics. In contrast, long biological DNA may be carried by microplastics to exert their biological functions. In this work, we only focused on the adsorption of DNA by microplastics. In turn, microplastics can help transport DNA and even protect the adsorbed DNA from degradation by nucleases, leading to biological effects. For example, it is known that graphene oxide can protect adsorbed DNA from nuclease digestion [36]. It would be interesting to compare microplastics with nanomaterials in such properties as a future research topic.

The second observation in this work is that transition metal ions such as Zn^{2+} and Mn^{2+} are more effective in promoting DNA adsorption compared to metals such as Mg^{2+}. In environmental water samples, although transition metal ions are likely to present in lower concentrations, they may still play an important role in promoting DNA adsorption. For example, in ocean water, typical Zn^{2+} and Mg^{2+} concentrations are up to 14 ppm and 1300 ppm, respectively [37,38]. In some industry wastewaters, high concentration of transition metal ions could be present along with high concentrations of plastics and microplastics. The added effect in attaching biological molecules including nucleic acids to plastics could be significant.

Finally, this study focused on fundamental adsorption studies in clean buffers. We also included a wastewater sample, in which microplastics also adsorbed DNA similar to that in the clean buffer. However, the composition of the wastewater sample is unknown and also hard to analyze. In real environmental water samples, there could be a range of molecules including proteins and they may compete for the surface of microplastics. Therefore, it would also be interesting to study the competition between proteins and DNA [39], which may have different mechanisms of adsorption based on their very different chemical structures.

4. Conclusions

Metal-mediated interactions are prominent for the adsorption and conjugation of DNA and various biomolecules onto nano- and micro-scale materials and surfaces [16,40,41]. We previously reported the effect of group 1A and 2A metal ions such as sodium and magnesium for the adsorption of oligonucleotides on microplastics. In this work, we studied the effect of transition metal ions on the adsorption of DNA, especially long biological DNA on microplastics. Transition metal ions including Zn^{2+} and Mn^{2+} showed a higher efficiency than Mg^{2+} for both ssDNA and dsDNA adsorption on microplastics likely due to their higher binding affinity to DNA. Metal-mediated interactions were vital for ssDNA on the microplastics. In addition, dsDNA (~2000 bp) adsorbed on microplastics even in the absence of metal ions likely due to the polyvalent interactions of multiple binding sites, which could amplify the weaker interactions to result in adsorption. Based on desorption experiments, hydrophobic interactions were responsible for dsDNA adsorption in the absence of metal ions. In addition, the adsorption affinity of the tested microplastics followed the order of PET > PS > PVC, possibly due to the extra attractive forces provided by the aromatic rings of PET and PS. Similar observations on DNA adsorption were also made in a wastewater sample. This work provides a fundamental understanding of environmental DNA adsorption on microplastics and facilitates future studies on aptamer selection for the detection of microplastics.

References

1. Geyer, R.; Jambeck, J.R.; Law, K.L. Production, Use, and Fate of All Plastics Ever Made. *Sci. Adv.* **2017**, *3*, e1700782. [CrossRef] [PubMed]
2. MacLeod, M.; Arp, H.P.H.; Tekman, M.B.; Jahnke, A. The Global Threat from Plastic Pollution. *Science* **2021**, *373*, 61–65. [CrossRef]
3. Ivleva, N.P. Chemical Analysis of Microplastics and Nanoplastics: Challenges, Advanced Methods, and Perspectives. *Chem. Rev.* **2021**, *121*, 11886–11936. [CrossRef] [PubMed]
4. Liu, S.; Huang, J.; Zhang, W.; Shi, L.; Yi, K.; Yu, H.; Zhang, C.; Li, S.; Li, J. Microplastics as a Vehicle of Heavy Metals in Aquatic Environments: A Review of Adsorption Factors, Mechanisms, and Biological Effects. *J. Environ. Manag.* **2022**, *302*, 113995. [CrossRef] [PubMed]
5. de Oliveira, T.T.S.; Andreu, I.; Machado, M.C.; Vimbela, G.; Tripathi, A.; Bose, A. Interaction of Cyanobacteria with Nanometer and Micron Sized Polystyrene Particles in Marine and Fresh Water. *Langmuir* **2020**, *36*, 3963–3969. [CrossRef]
6. Ju, S.; Shin, G.; Lee, M.; Koo, J.M.; Jeon, H.; Ok, Y.S.; Hwang, D.S.; Hwang, S.Y.; Oh, D.X.; Park, J. Biodegradable Chito-Beads Replacing Non-Biodegradable Microplastics for Cosmetics. *Green Chem.* **2021**, *23*, 6953–6965. [CrossRef]
7. Wright, S.L.; Kelly, F.J. Plastic and Human Health: A Micro Issue? *Environ. Sci. Technol.* **2017**, *51*, 6634–6647. [CrossRef]
8. Cox, K.D.; Covernton, G.A.; Davies, H.L.; Dower, J.F.; Juanes, F.; Dudas, S.E. Human Consumption of Microplastics. *Environ. Sci. Technol.* **2019**, *53*, 7068–7074. [CrossRef]
9. Hildebrandt, L.; Nack, F.; Zimmermann, T.; Pröfrock, D. Microplastics as a Trojan Horse for Trace Metals. *J. Hazard. Mater. Lett.* **2021**, *2*, 100035. [CrossRef]
10. Lee, A.; Mondon, J.; Merenda, A.; Dumée, L.F.; Callahan, D.L. Surface Adsorption of Metallic Species onto Microplastics with Long-Term Exposure to the Natural Marine Environment. *Sci. Total Environ.* **2021**, *780*, 146613. [CrossRef]
11. Zhang, Y.; Su, X.; Tam, N.F.; Lao, X.; Zhong, M.; Wu, Q.; Lei, H.; Chen, Z.; Li, Z.; Fu, J. An Insight into Aggregation Kinetics of Polystyrene Nanoplastics Interaction with Metal Cations. *Chin. Chem. Lett.* **2022**, *33*, 5213–5217. [CrossRef]
12. Cao, Y.; Zhao, M.; Ma, X.; Song, Y.; Zuo, S.; Li, H.; Deng, W. A Critical Review on the Interactions of Microplastics with Heavy Metals: Mechanism and Their Combined Effect on Organisms and Humans. *Sci. Total Environ.* **2021**, *788*, 147620. [CrossRef] [PubMed]
13. Zhou, W.; Saran, R.; Liu, J. Metal Sensing by DNA. *Chem. Rev.* **2017**, *117*, 8272–8325. [CrossRef] [PubMed]
14. Wang, Z.; Xie, Y.; Li, Y.; Huang, Y.; Parent, L.R.; Ditri, T.; Zang, N.; Rinehart, J.D.; Gianneschi, N.C. Tunable, Metal-Loaded Polydopamine Nanoparticles Analyzed by Magnetometry. *Chem. Mater.* **2017**, *29*, 8195–8201. [CrossRef]
15. Valencia, L.; Monti, S.; Kumar, S.; Zhu, C.; Liu, P.; Yu, S.; Mathew, A.P. Nanocellulose/Graphene Oxide Layered Membranes: Elucidating Their Behaviour During Filtration of Water and Metal Ions in Real Time. *Nanoscale* **2019**, *11*, 22413–22422. [CrossRef]
16. Kushalkar, M.P.; Liu, B.; Liu, J. Promoting DNA Adsorption by Acids and Polyvalent Cations: Beyond Charge Screening. *Langmuir* **2020**, *36*, 11183–11195. [CrossRef]
17. Zandieh, M.; Liu, J. Metal-Doped Polydopamine Nanoparticles for Highly Robust and Efficient DNA Adsorption and Sensing. *Langmuir* **2021**, *37*, 8953–8960. [CrossRef]
18. Wang, Z.; Huang, Z.; Han, J.; Xie, G.; Liu, J. Polyvalent Metal Ion Promoted Adsorption of DNA Oligonucleotides by Montmorillonite. *Langmuir* **2021**, *37*, 1037–1044. [CrossRef]

19. Zandieh, M.; Patel, K.; Liu, J. Adsorption of Linear and Spherical DNA Oligonucleotides onto Microplastics. *Langmuir* **2022**, *38*, 1915–1922. [CrossRef]
20. Dunn, M.R.; Jimenez, R.M.; Chaput, J.C. Analysis of Aptamer Discovery and Technology. *Nat. Rev. Chem.* **2017**, *1*, 76. [CrossRef]
21. Zhou, Y.; Huang, Z.; Yang, R.; Liu, J. Selection and Screening of DNA Aptamers for Inorganic Nanomaterials. *Chem. Eur. J.* **2018**, *24*, 2525–2532. [CrossRef] [PubMed]
22. Yu, H.; Alkhamis, O.; Canoura, J.; Liu, Y.; Xiao, Y. Advances and Challenges in Small-Molecule DNA Aptamer Isolation, Characterization, and Sensor Development. *Angew. Chem. Int. Ed.* **2021**, *60*, 16800–16823. [CrossRef] [PubMed]
23. Li, Y.; Gao, H.; Qi, Z.; Huang, Z.; Ma, L.; Liu, J. Freezing-Assisted Conjugation of Unmodified Diblock DNA to Hydrogel Nanoparticles and Monoliths for DNA and Hg^{2+} Sensing. *Angew. Chem. Int. Ed.* **2021**, *60*, 12985–12991. [CrossRef] [PubMed]
24. Zandieh, M.; Liu, J. Removal and Degradation of Microplastics Using the Magnetic and Nanozyme Activities of Bare Iron Oxide Nanoaggregates. *Angew. Chem. Int. Ed.* **2022**, *61*, e202212013. [CrossRef]
25. Hulme, E.C.; Trevethick, M.A. Ligand Binding Assays at Equilibrium: Validation and Interpretation. *Br. J. Pharmacol.* **2010**, *161*, 1219–1237. [CrossRef]
26. Yu, D.; Mou, H.; Zhao, X.; Wang, Y.; Mu, T. Eutectic Molecular Liquids Based on Hydrogen Bonding and π–π Interaction for Exfoliating Two-Dimensional Materials and Recycling Polymers. *Chem. Asian J.* **2019**, *14*, 3350–3356. [CrossRef]
27. Ni, Y.-P.; Li, Q.-T.; Chen, L.; Wu, W.-S.; Qin, Z.-H.; Zhang, Y.; Chen, L.; Wang, X.-L.; Wang, Y.-Z. Semi-Aromatic Copolyesters with High Strength and Fire Safety Via Hydrogen Bonds and Π-Π Stacking. *Chem. Eng. J.* **2019**, *374*, 694–705. [CrossRef]
28. Zandieh, M.; Liu, J. Transition Metal-Mediated DNA Adsorption on Polydopamine Nanoparticles. *Langmuir* **2020**, *36*, 3260–3267. [CrossRef]
29. Zandieh, M.; Liu, J. Cooperative Metal Ion-Mediated Adsorption of Spherical Nucleic Acids with a Large Hysteresis. *Langmuir* **2020**, *36*, 14324–14332. [CrossRef]
30. Dong, H.; Chen, Y.; Wang, J.; Zhang, Y.; Zhang, P.; Li, X.; Zou, J.; Zhou, A. Interactions of Microplastics and Antibiotic Resistance Genes and Their Effects on the Aquaculture Environments. *J. Hazard. Mater.* **2021**, *403*, 123961. [CrossRef]
31. Yuan, Q.; Sun, R.; Yu, P.; Cheng, Y.; Wu, W.; Bao, J.; Alvarez, P.J. UV-Aging of Microplastics Increases Proximal ARG Donor-Recipient Adsorption and Leaching of Chemicals That Synergistically Enhance Antibiotic Resistance Propagation. *J. Hazard. Mater.* **2022**, *427*, 127895. [CrossRef]
32. Glasel, J. Validity of Nucleic Acid Purities Monitored by 260nm/280nm Absorbance Ratios. *BioTechniques* **1995**, *18*, 62–63.
33. Lucena-Aguilar, G.; Sánchez-López, A.M.; Barberán-Aceituno, C.; Carrillo-Avila, J.A.; López-Guerrero, J.A.; Aguilar-Quesada, R. DNA Source Selection for Downstream Applications Based on DNA Quality Indicators Analysis. *Biopreserv. Biobank.* **2016**, *14*, 264–270. [CrossRef] [PubMed]
34. Liu, B.; Sun, Z.; Zhang, X.; Liu, J. Mechanisms of DNA Sensing on Graphene Oxide. *Anal. Chem.* **2013**, *85*, 7987–7993. [CrossRef] [PubMed]
35. Mammen, M.; Choi, S.K.; Whitesides, G.M. Polyvalent Interactions in Biological Systems: Implications for Design and Use of Multivalent Ligands and Inhibitors. *Angew. Chem. Int. Ed.* **1998**, *37*, 2754–2794. [CrossRef]
36. Lu, C.-H.; Zhu, C.-L.; Li, J.; Liu, J.-J.; Chen, X.; Yang, H.-H. Using Graphene to Protect DNA from Cleavage During Cellular Delivery. *Chem. Commun.* **2010**, *46*, 3116–3118. [CrossRef]
37. Rollion-Bard, C.; Saulnier, S.; Vigier, N.; Schumacher, A.; Chaussidon, M.; Lécuyer, C. Variability in Magnesium, Carbon and Oxygen Isotope Compositions of Brachiopod Shells: Implications for Paleoceanographic Studies. *Chem. Geol.* **2016**, *423*, 49–60. [CrossRef]
38. Andersen, M.B.; Vance, D.; Archer, C.; Anderson, R.F.; Ellwood, M.J.; Allen, C.S. The Zn Abundance and Isotopic Composition of Diatom Frustules, a Proxy for Zn Availability in Ocean Surface Seawater. *Earth Planet. Sci. Lett.* **2011**, *301*, 137–145. [CrossRef]
39. Liu, B.; Ma, L.; Huang, Z.; Hu, H.; Wu, P.; Liu, J. Janus DNA Orthogonal Adsorption of Graphene Oxide and Metal Oxide Nanoparticles Enabling Stable Sensing in Serum. *Mater. Horiz.* **2018**, *5*, 65–69. [CrossRef]
40. Tong, F.; Liu, D.; Zhang, Z.; Chen, W.; Fan, G.; Gao, Y.; Gu, X.; Gu, C. Heavy Metal-Mediated Adsorption of Antibiotic Tetracycline and Ciprofloxacin on Two Microplastics: Insights into the Role of Complexation. *Environ. Res.* **2023**, *216*, 114716. [CrossRef]
41. Hao, J.; Mokhtari, M.; Pedreira-Segade, U.; Michot, L.J.; Daniel, I. Transition Metals Enhance the Adsorption of Nucleotides onto Clays: Implications for the Origin of Life. *ACS Earth Space Chem.* **2018**, *3*, 109–119. [CrossRef]